Interferences of real trajectories and the emergence of quantum features in electron-atom scattering in a strong laser field

A. Čerkić[1] and D. B. Milošević[2,3]
[1]*Federal Meteorological Institute, Bardakčije 12, 71000 Sarajevo, Bosnia and Herzegovina*
[2]*Faculty of Science, University of Sarajevo, Zmaja od Bosne 35, 71000 Sarajevo, Bosnia and Herzegovina*
[3]*Max-Born-Institut, Max-Born-Strasse 2a, 12489 Berlin, Germany*
(Received 17 October 2005; published 9 March 2006)

Using the example of electron-atom scattering in a strong laser field, it is shown that the oscillatory structure of the scattered electron spectrum can be explained as a consequence of the interference of the real electron trajectories in terms of Feynman's path integral. While in previous work on quantum-orbit theory the complex solutions of the saddle-point equations were considered, we show here that for the electron-atom scattering with much simpler real solutions a satisfactory agreement with the strong-field-approximation results can be achieved. Real solutions are applicable both for the direct (low-energy) and the rescattering (high-energy) plateau in the scattered electron spectrum. In between the plateaus and beyond the rescattering cutoff good results can be obtained using the complex (quantum) solutions and the uniform approximation. The interference of real solutions is related to the recent attosecond double-slit experiment in time.

DOI: 10.1103/PhysRevA.73.033413 PACS number(s): 34.80.Qb, 34.50.Rk, 32.80.Wr, 42.50.Hz

I. INTRODUCTION

Atomic and molecular processes in a strong laser field have received a lot of attention during the past few decades [1–3]. In these processes electrons and photons of high energies are emitted. Since the laser field is strong there is a phase of these processes during which the electrons can be considered as moving in the laser field only. This leads to a theoretical approach named the strong-field approximation (SFA). For example, in the case of ionization of atoms by a strong laser field this approximation includes the neglect of the interaction of the ionized electron with its parent ion. This is the famous Keldysh approximation [4]. If the laser field is strong enough, the ionized electron is able to return to the parent ion and to scatter on it. Theories that include such rescattering were developed and using them it was possible to explain experimentally observed plateaus in the photon and electron spectra [1,2,5].

Particularly useful was the approach that uses Feynman's path integral formalism and the concept of quantum orbits ([1,6,7] and references therein). In the quantum-orbit theory the initial step of the process (for ionization this is the tunneling) has the quantum nature, and the initial time is complex. Introducing such complex time into the classical equation of motion, one obtains that the electron is "born" at the end of the tunnel (usually a few atomic units away from the nucleus), and then is leaded by the laser field. The total probability amplitude of the corresponding process is a coherent sum of the contributions of all these paths with the complex times. Therefore, the quantum nature of atomic processes in a strong laser field is expressed by the complex time and by the interference of quantum orbits. Mathematically, the complex time emerges from the saddle-point solutions for which the classical action is stationary. For example, for the above-threshold ionization this condition is expressed as the energy-conserving condition at the ionization time: the negative initial electron energy $E_i=-I_p$ (I_p is the ionization potential) has to be equal to the positive electron kinetic energy in the laser field $E_{\mathbf{k}}=[\mathbf{k}+\mathbf{A}(t_i)]^2/2$, where $\mathbf{k}$ is the final observed electron momentum and $\mathbf{A}(t_i)$ is the vector potential of the laser field at the ionization time t_i (we use the atomic system of units $e=\hbar=m=1$). The solutions of the equation $E_i=E_{\mathbf{k}}$ exist only for the complex time t_i.

Let us now consider a different atomic process: electron-atom scattering in a laser field (see, for example [8], and references therein). In this case, the initial electron kinetic energy $E_{\mathbf{k}_i}=\mathbf{k}_i^2/2$ is positive and real solutions of the saddle-point equations exist. Therefore, the electron can follow the real trajectory. The quantum nature of such processes in strong fields comes through the interference (in the sense of the Feynman's path integral) of the amplitudes that correspond to these real electron trajectories. An approach that takes into account only the real trajectories is simpler than the quantum-orbit formalism [1,6,7] and has already been used to qualitatively analyze high-order above-threshold ionization by few-cycle pulses [9,10]. It should be mentioned that this approach was not based on the *S*-matrix formalism, which we will use in the present paper. Instead, solving the classical Newton equation of motion, the rescattering real electron trajectories were obtained and used to qualitatively explain the multiplateau structure and the cutoff in the electron energy spectrum. However, more recently, quantum-orbit formalism with complex saddle-point solutions has been developed for high-order above-threshold ionization by few-cycle pulses [11]. It was shown that the real-trajectory formalism fails to reproduce the SFA results and that even the cutoff positions are significantly shifted from their classical values [12,13].

Our aim in the present paper is to show that there are the processes for which the theory with real times and real electron trajectories can give excellent agreement with the SFA results. For this purpose we will use recently considered laser-assisted electron-atom scattering [14]. Two plateaus, within which the scattering cross section as a function of the

scattered electron energy is of the same order of magnitude, the direct and the rescattering plateau, were observed. We will show that both these plateaus can be described very well using the real-trajectory formalism. Both plateaus finish with the corresponding cutoff, after which the scattering cross section rapidly decreases with the increase of the final electron kinetic energy. We will show that in the region between the plateaus, and beyond the second plateau the real-trajectory method cannot be applied and that the quantum-orbit theory is necessary. After a brief presentation of the theory of laser-assisted potential scattering in Sec. II in Sec. III we consider the direct scattering. In Sec. IV we analyze the laser-induced rescattering, and, finally, in Sec. V the conclusions and comments are given.

II. THEORY

The S-matrix element for scattering of electrons on a short-range potential $V(\mathbf{r})$ in the presence of a laser field can be written in the form [14]

$$S_{fi} = -2\pi i \sum_{n>-E_{\mathbf{k}_i}/\omega}^{\infty} \delta(E_{\mathbf{k}_f} - E_{\mathbf{k}_i} - n\omega) T_{fi}(n), \tag{1}$$

where the delta function expresses the energy-conserving condition: the final electron kinetic energy $E_{\mathbf{k}_f}=\mathbf{k}_f^2/2$ is equal to the sum of the initial electron kinetic energy $E_{\mathbf{k}_i}$ and n times the photon energy ω (the sum runs over all open channels with $E_{\mathbf{k}_f}>0$). The T-matrix element $T_{fi}(n)$ describes the free-free electron transitions with the exchange of n photons with the laser field. This can be either absorption (for $n>0$) or emission (for $n<0$). The T-matrix element can be written in the form of the Born expansion in the scattering potential $V(\mathbf{r})$,

$$T_{fi}(n) = T_{fi}^{1\mathrm{B}}(n) + T_{fi}^{2\mathrm{B}}(n) + \cdots . \tag{2}$$

In Ref. [14] it was shown that the first Born approximation corresponds to the direct scattering, while the second Born approximation describes the rescattering, i.e., the three-step process in which the electron, after the first scattering, moves in the laser field and returns to the atom (second step), and, in the third step, rescatters on it. In this sense, the laser-assisted electron-atom scattering, within the first and the second Born approximation, is analogous to the high-order laser-induced atomic processes such as high-order above-threshold ionization and high-order harmonic generation, which can be treated using the strong-field approximation. Therefore, our approach can be considered as the SFA applied to the free-free transitions [15]. In Ref. [14] the scattering of electrons on inert gases was considered and the scattering potential was modeled by the sum of the polarization potential and the double Yukawa potential, while the interaction with the laser field was taken into account exactly using the Gordon-Volkov solution of the Schrödinger equation for the electron in the laser field [8]. We have checked that the above formulation, in the dipole approximation, leads to the same results both in the length gauge and the velocity gauge. This is important in the context of the recent findings that the length gauge should be used in applications of the SFA to the above-threshold ionization [16].

The direct T-matrix element can be written in the form

$$T_{fi}^{\mathrm{D}}(n) = T_{fi}^{1\mathrm{B}}(n) = V_{\mathbf{q}} \int_0^T \frac{dt}{T} \exp[iS_n^{\mathrm{D}}(t)], \tag{3}$$

where the upper index D denotes the direct scattering, $T=2\pi/\omega$ is the period of the laser field, and $V_{\mathbf{q}}=(2\pi)^{-3}\int V(\mathbf{r})e^{i\mathbf{q}\cdot\mathbf{r}}\,d^3\mathbf{r}$, $\mathbf{q}=\mathbf{k}_i-\mathbf{k}_f$, is the Fourier transform of the potential $V(\mathbf{r})$. The classical action for the direct scattering with absorption of n photons from the laser field is

$$S_n^{\mathrm{D}}(t) = n\omega t - \boldsymbol{\alpha}(t)\cdot\mathbf{q} = S_{\mathbf{k}_f}(t) - S_{\mathbf{k}_i}(t), \tag{4}$$

with $\boldsymbol{\alpha}(t)=\int^t \mathbf{A}(t')dt'$ and $S_{\mathbf{k}}(t)=\frac{1}{2}\int^t dt'[\mathbf{k}+\mathbf{A}(t')]^2$. For a linearly polarized monochromatic laser field with the vector potential $\mathbf{A}(t)=\hat{\mathbf{e}}A_0\cos\omega t$, using the integral representation of the ordinary Bessel function of the integer order n, $J_n(x)$ [17], for the direct T-matrix element we obtain

$$T_{fi}^{\mathrm{D}}(n) = V_{\mathbf{q}} J_n(x), \tag{5}$$

where $x=(A_0/\omega)\hat{\mathbf{e}}\cdot\mathbf{q}$. This is the well-known Bunkin and Fedorov result [18].

The rescattering T-matrix element, i.e., the second Born approximation, can be written in the form of a five-dimensional integral [14]. The three-dimensional integral over the intermediate electron momenta $\mathbf{k}$ can be solved analytically. In this case, the momentum $\mathbf{k}$ is replaced with the stationary momentum

$$\mathbf{k}_s = -\int_t^{t+\tau} \mathbf{A}(t')dt'/\tau = [\boldsymbol{\alpha}(t) - \boldsymbol{\alpha}(t+\tau)]/\tau,$$

and only the two-dimensional integral over the first scattering time t and over the traveling time τ between the first scattering and the rescattering remains, so that

$$T_{fi}^{\mathrm{R}}(n) = T_{fi}^{2\mathrm{B}}(n) = \int_0^T \frac{dt}{T} \int_0^\infty d\tau \left(\frac{2\pi}{i\tau}\right)^{3/2} \times V_{\mathbf{k}_s-\mathbf{k}_f} V_{\mathbf{k}_i-\mathbf{k}_s} \exp[iS_n^{\mathrm{R}}(t,\tau)]. \tag{6}$$

Here $S_n^{\mathrm{R}}(t,\tau)$ is the rescattering classical action

$$\begin{aligned} S_n^{\mathrm{R}}(t,\tau) &= n\omega t - \boldsymbol{\alpha}(t)\cdot\mathbf{q} + (\mathbf{k}_f - \mathbf{k}_s)^2\tau/2 \\ &= S_{\mathbf{k}_f}(t+\tau) - S_{\mathbf{k}_s}(t+\tau) + S_{\mathbf{k}_s}(t) - S_{\mathbf{k}_i}(t). \end{aligned} \tag{7}$$

The differential cross section for scattering of an electron with the initial momentum $\mathbf{k}_i$ on a local potential $V(\mathbf{r})$, so that the final electron momentum is $\mathbf{k}_f$ and that n photons are exchanged with the laser field, is defined by

$$\frac{d\sigma_{fi}(n)}{d\Omega} = (2\pi)^4 \frac{k_f}{k_i} |T_{fi}(n)|^2. \tag{8}$$

For a spherically symmetric problem the results are independent on the polar angle ϕ_f of the final electron momentum $\mathbf{k}_f \equiv (k_f, \theta_f, \phi_f)$. In the present paper we will consider only the following scattering geometry: The incident electron momentum $\mathbf{k}_i$ is in the direction of the laser field polarization

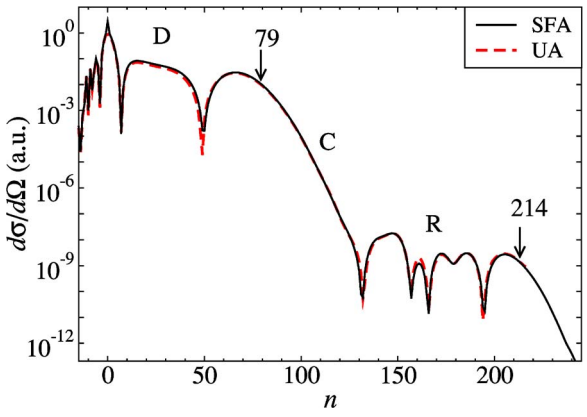

FIG. 1. (Color online) The differential cross section for potential scattering of electrons having the initial kinetic energy $E_{\mathbf{k}_i}=18$ eV on He atoms in the presence of a monochromatic linearly polarized laser field, as a function of the number of photons n exchanged with the laser field. The laser wavelength is 1060 nm and the intensity 2.6×10^{14} W/cm^2. The incident electron momentum is in the direction of the laser field polarization, and the forward scattering is considered. The direct (D) and the rescattering (R) plateaus with the corresponding cutoffs at $n_D=79$ and $n_R=214$ are denoted in the figure. The results obtained using the strong-field approximation (SFA) are compared with the results obtained using the uniform approximation (UA) with the real solutions of the stationary-point equations for the direct and the rescattering plateau and with the complex solutions in the transition region between the plateaus (C).

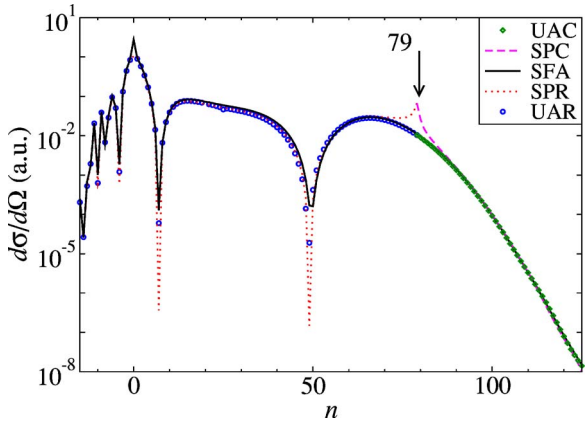

FIG. 2. (Color online) A comparison of the numerical results for the direct part of the differential cross section obtained using different methods. The laser, atomic, and the incident electron parameters are the same as in Fig. 1.

$\hat{\mathbf{e}}$, i.e., $\hat{\mathbf{k}}_i\cdot\hat{\mathbf{e}}=1$, while the angle between the scattered electron momentum $\mathbf{k}_f$ and the direction of the laser field is $\theta_f=0$ (forward scattering).

The differential cross section can be calculated numerically using the method described in Ref. [14]. In Fig. 1 we present a characteristic example of the numerical results for the potential scattering on He atoms in a linearly polarized monochromatic laser field. The differential cross section as a function of the number of photons exchanged with the laser field exhibits two plateaus: the direct plateau, with the corresponding cutoff at $n_D=79$, and the rescattering plateau, which is six orders of magnitude lower and has the cutoff at $n_R=214$. We will use this example in order to illustrate the method of real trajectories and its limitation.

III. DIRECT SCATTERING

Let us first analyze the direct T-matrix element. We have already shown that it can be written in the simple form (5). For the scattering geometry used in our example, we have $x=A_0k_i(1-\sqrt{1+n\omega/E_{\mathbf{k}_i}})/\omega<0$ for $n>0$. Furthermore, for the example presented in Fig. 1 the number n can be large, and we also have $A_0k_i/\omega=53.6$, so that $|x|$ is large. Supposing that $n=|x|\cos\beta$, using the Debye asymptotic expansion of the Bessel functions [17] we obtain

$$J_n(x)\approx\frac{(-1)^n}{\sqrt{2\pi|x|\sin\beta}}(e^{i\psi}+e^{-i\psi}), \tag{9}$$

with $\psi=|x|\sin\beta-n\beta-\pi/4$. We see that, in this case, the direct T matrix, Eqs. (5) and (9), is expressed as a sum of the two terms whose interference is responsible for the oscillations that appear in the direct plateau in Fig. 1. It is indicative that the argument $|x|$ becomes smaller than n for $n=79$, which is exactly the cutoff position of the direct plateau presented in Fig. 1.

Let us now relate this result to the real electron trajectories. We will start from the more general case, Eqs. (3) and (4). The integral over the time t can be solved using the saddle-point method. If the time t is considered as real, this method reduces to the stationary phase method [19,20]. In this case, from the condition that the first derivative over the time t of the action $S_n^D(t)$ is equal to zero, for the direct scattering we obtain the equation

$$[\mathbf{k}_i+\mathbf{A}(t)]^2=[\mathbf{k}_f+\mathbf{A}(t)]^2, \tag{10}$$

which expresses the electron energy conserving condition at the scattering time t. The real solutions $t=t_s$ of the above equation are the stationary points. If we apply the stationary phase method, we obtain

$$T_{fi}^D(n)\approx\frac{V_{\mathbf{q}}}{T}\sum_{t_s}\left(\frac{2\pi}{|S_n''(t_s)|}\right)^{1/2}e^{i[S_n^D(t_s)+\delta\pi/4]}, \tag{11}$$

where the sum is over all stationary points t_s, and

$$S_n''(t_s)=\partial^2S_n^D(t_s)/\partial t^2,\quad \delta=\mathrm{sgn}[S_n''(t_s)]. \tag{12}$$

For the parameters of Fig. 1, for each n, there are two stationary points t_1 and $t_2=T-t_1$ that are symmetric with respect to $t=T/2$. The real solutions t_1 and t_2 exist only for $n<n_D=79$. Introducing these solutions into Eqs. (11) and (8), we have calculated the differential cross section. In Fig. 2 this result is presented by a dotted line (denoted by SPR—the stationary phase method with the real solutions). We see that this result agrees very well with the result obtained by numerical integration (SFA—solid line) for lower values of n. With the increase of n, the two solutions t_1 and t_2 become closer to each other. When n approaches $n_D=79$ the SPR method fails (see the dotted line spike below

$n=79$; this is a consequence of the inadequacy of the saddle-point approximation for the case of two coalescing saddle points, as we will explain later).

For $n=n_{\mathrm{D}}$ there is only one real stationary solution $t_1=t_2=T/2$, while for $n>n_{\mathrm{D}}$ there are no more real solutions. However, the two complex solutions appear: $t_1=T/2+ia$, $t_2=T/2-ia$, $a>0$, and we should use the saddle-point method instead of the stationary phase method. Equations (11) and (12) remain valid for the saddle-point method, except that the times t_s are now complex and $\delta=\mathrm{sgn}[\mathrm{Im}\, S_n''(t_s)]$. The problem is that the contribution of the solution $t_2=T/2-ia$, which corresponds to $\delta=-1$, is divergent: it increases with the increase of n and should be neglected as unphysical. Keeping only the solution $t_1=T/2+ia$, with $\mathrm{Im}\, t_1>0$ and $\delta=1$, and using Eqs. (8) and (11), we have calculated the differential cross section for $n>n_{\mathrm{D}}$. The result is presented in Fig. 2 by a dashed line (denoted by SPC: the saddle-point method with the complex solutions). Therefore, we were able to reproduce the SFA result using the saddle-point approximation, which includes: (i) for $n<n_{\mathrm{D}}$ the interference of two contributions corresponding to the solutions of the equation that expresses the energy-conserving condition over the real scattering times t, (ii) for $n>n_{\mathrm{D}}$ (beyond the direct cutoff) only one, exponentially decreasing, contribution that corresponds to the complex time with $\mathrm{Im}\, t>0$.

The interference of contributions having real times can be illustrated by presenting the real electron trajectories that are the solutions of the classical Newton equation of motion for the electron in the laser field $\ddot{\mathbf{r}}(t)=-\mathbf{E}(t)$, with $\mathbf{E}(t)=-\partial\mathbf{A}(t)/\partial t$ the laser electric field vector. The initial electron momentum is $\mathbf{k}_i$ and the field is turned on at the time $t=t_i$ when the electron position $\mathbf{r}(t_i)$ is such that the electron elastically scatters on the atom at the time t_s. The electron trajectory for $t_i<t<t_s$ is

$$\mathbf{r}(t)=\int_{t_i}^{t}dt'\,\mathbf{A}(t')+[\mathbf{k}_i-\mathbf{A}(t_i)](t-t_i)+\mathbf{r}(t_i). \qquad (13)$$

The electron velocity at the moment of scattering ($t=t_s$) is $\mathbf{v}(t_s)=\mathbf{k}_i+\mathbf{A}(t_s)-\mathbf{A}(t_i)$. The sign of this velocity is changed after the scattering. Thus, for $t>t_s$ we have

$$\mathbf{r}(t)=\int_{t_s}^{t}dt'\,\mathbf{A}(t')+[\mathbf{A}(t_i)-2\mathbf{A}(t_s)-\mathbf{k}_i](t-t_s)+\mathbf{r}(t_s), \qquad (14)$$

where $\mathbf{r}(t_s)=\mathbf{0}$ (the scattering occurs at the origin). The final electron momentum outside the laser field is $\mathbf{k}_f$ since the time t_s satisfies Eq. (10).

An example of these trajectories is presented in Fig. 3. For the direct scattering, two electron trajectories contribute to the same electron energy $E_{\mathbf{k}_f}=E_{\mathbf{k}_i}+n\omega$ ($n=60$ in the presented case), registered at the detector. The electron will have this energy only if it scatters at time t_1 or at time t_2. This is an analog of the double-slit experiment in time that was recently demonstrated in the above-threshold ionization experiment with a few-cycle laser field [21]. In this experiment, by changing the carrier-envelope phase, it was possible

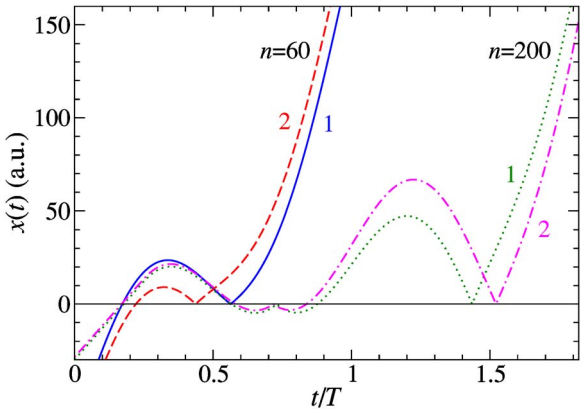

FIG. 3. (Color online) Trajectories of the electron in the laser field for the parameters of Fig. 1. The direct-scattering trajectories (solid and dashed line) for $n=60$ and the rescattering trajectories (dotted and dot-dashed line) for $n=200$ are presented. The rescattering trajectories correspond to the solutions having the highest maximum in Fig. 4, denoted by $p=1$.

to open only one or two windows in time and to control the process. Similarly, here we have two windows in time centered at t_1 and t_2 for which we will observe the scattered electrons with the energy $E_{\mathbf{k}}\approx E_{\mathbf{k}_f}$.

From Fig. 2 we see that the saddle-point method fails near $n=n_{\mathrm{D}}$ (see the spike formed by the SPR dotted curve and the SPC dashed curve). The reason is that the two stationary points t_1 and t_2 of the integral over t in Eq. (3) approach the common limit t_c when the final electron energy $E_{\mathbf{k}_f}$ approaches the value $E_c=E_{\mathbf{k}_i}+n_{\mathrm{D}}\omega$, which causes the breakdown of the standard saddle-point approximation. One can say that the asymptotic expansion formula (11), obtained according to the algorithm of the standard stationary phase method, is nonuniform with respect to $E_{\mathbf{k}_f}$. In the theory of asymptotic expansions, there is a method that can cure the problem: the uniform approximation for the case of two coalescing saddle points [19,20]. The action (4) in Eq. (3) is expanded in the neighborhood of these two saddle points, higher order terms are taken into account, and the resulting integrals are combined as the collective contribution of both saddle points. The final expression can be cast in a simple form, which uses the same information as the standard saddle-point method, i.e., the solutions of Eq. (10). For the direct scattering, there is only one such pair of solutions, and the T-matrix element $T_{fi}^{\mathrm{D}}(n)$ in the uniform approximation can be written as

$$T_{fi}^{\mathrm{D}}(n)\approx 2^{1/2}\pi[b_{n+}\,\mathrm{Ai}(\xi_n)+ib_{n-}\,\mathrm{Ai}'(\xi_n)]e^{i\bar{S}_n}, \qquad (15)$$

where Ai and Ai′ are the Airy function and its first derivative, respectively, and

$$\bar{S}_n=[S_n^{\mathrm{D}}(t_1)+S_n^{\mathrm{D}}(t_2)]/2,$$

$$\xi_n=-\eta_n\{3[S_n^{\mathrm{D}}(t_1)-S_n^{\mathrm{D}}(t_2)]/4\}^{2/3}, \qquad (16)$$

$$b_{n\pm} = \xi^{\pm 1/4} \frac{V_{\mathbf{k}_i-\mathbf{k}_f}}{T} [|S_n''(t_1)|^{-1/2} \pm |S_n''(t_2)|^{-1/2}], \qquad (17)$$

where $\eta_n=1$ for $n \leqslant n_D$ and $\eta_n=\exp(-i2\pi/3)$ for $n>n_D$, while S_n^D and S_n'' are given by Eqs. (4) and (12), respectively. The above result is valid both for $n \leqslant n_D$ (real solutions t_1 and $t_2=T-t_1$) and for $n>n_D$ (complex solutions $t_{1,2}=T/2\pm ia$; we do not neglect the solution t_2, as we have done for the saddle-point method). From Fig. 2 we see that the agreement with the SFA result is excellent, both for the uniform approximation with the real solutions (UAR—circles; $n \leqslant n_D$) and for the uniform approximation with the complex solutions (UAC—diamonds; $n>n_D$).

IV. RESCATTERING

The integrals that appear in the rescattering T-matrix element (6) can also be solved using the asymptotic expansion of integrals. The situation is more complicated since we have a two-dimensional integral over the first scattering time t and the traveling time τ. The stationary points $\{t_s, \tau_s\}$ can be found solving the system of equations $\partial S_n^R(t,\tau)/\partial t=0$ and $\partial S_n^R(t,\tau)/\partial \tau=0$, where the rescattering classical action $S_n^R(t,\tau)$ is given by Eq. (7). This system of equations has the form of the energy conserving conditions at the first scattering time t and at the rescattering time $t+\tau$,

$$[\mathbf{k}_i + \mathbf{A}(t)]^2 = [\mathbf{k}_s + \mathbf{A}(t)]^2, \qquad (18)$$

$$[\mathbf{k}_f + \mathbf{A}(t+\tau)]^2 = [\mathbf{k}_s + \mathbf{A}(t+\tau)]^2. \qquad (19)$$

The stationary intermediate electron momentum $\mathbf{k}_s$ is given previously, Eq. (6). Physically, $\mathbf{k}_s$ is defined by the condition that the electron, having the momentum $\mathbf{k}_s$, after the first scattering at the time t, returns to the same position at the time $t+\tau$, $\mathbf{r}(t+\tau)=\mathbf{r}(t)$, following the trajectory that is the solution of the Newton equation for the electron in the laser field $\ddot{\mathbf{r}}(t)=-\mathbf{E}(t)$.

The stationary-point approximation for the two-dimensional integral (6) can be written in the form

$$T_{fi}^R(n) \approx \frac{4\pi}{T}(i-1) \sum_{\{t_s,\tau_s\}} \frac{V_{\mathbf{k}_s-\mathbf{k}_f} V_{\mathbf{k}_i-\mathbf{k}_s}}{|\det[C_n(t_s,\tau_s)]|^{1/2}} \times (\pi/\tau_s)^{3/2} \exp\{i[S_n^R(t_s,\tau_s) + \delta\pi/2]\}, \qquad (20)$$

where the sum is over the stationary points $\{t_s, \tau_s\}$,

$$C_n(t_s,\tau_s) = \begin{bmatrix} S_n^{tt}(t_s,\tau_s) & S_n^{t\tau}(t_s,\tau_s) \\ S_n^{\tau t}(t_s,\tau_s) & S_n^{\tau\tau}(t_s,\tau_s) \end{bmatrix}, \qquad (21)$$

$S_n^{\sigma\rho}(t_s,\tau_s)=\partial^2 S_n^R(t_s,\tau_s)/\partial\sigma\partial\rho$, and $\delta=1$, if both eigenvalues of the matrix $C_n(t_s,\tau_s)$ are positive, $\delta=0$, if they have opposite signs, and $\delta=-1$, if both are negative.

For a fixed value of n the solutions of the system of Eqs. (18) and (19) come in pairs, which we will denote by $\{t_j^p, \tau_j^p\}$, $j=1,2$, $p=1,2,3,\ldots$. The index j denotes the members of each pair, while the index p counts the different pairs. An example of these solutions is presented in Fig. 4. The solutions $\{t_j^p, \tau_j^p\}$ are classified according to the values of τ so that $\tau_j^1 < \tau_j^2 < \tau_j^3 < \cdots$ and $\tau_1^p < \tau_2^p$. Besides the so classified solutions there are more rescattering solutions for $\tau < T/2$ (denoted by R in the figure). The maximum value of n for these solutions is below the cutoff value of the direct scattering, so that their contribution to the differential cross section can be neglected [22]. From Fig. 4 we see that for each pair p there is a cutoff value $n=n_R^p$, after which there are no more real solutions.

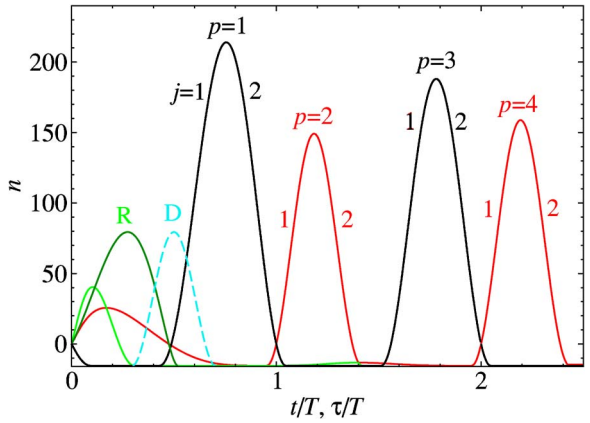

FIG. 4. (Color online) The solutions of the stationary-point equations (18) and (19) for the parameters of Fig. 1. The number of photons n exchanged with the laser field is presented as a function of the travel time τ, expressed in optical periods T. The solutions for the direct scattering (dashed line, denoted by D) are presented as a function of the first scattering time t, $0<t/T<1$. For the rescattering there are more solutions that are classified by the numbers j and p, as explained in the text.

In Fig. 5 the results for the differential cross section as a function of the number of photons exchanged with the laser field obtained using the strong-field approximation (solid line) are compared with the results obtained using the stationary phase approximation (dashed line). For the approximate results only the real rescattering solutions with

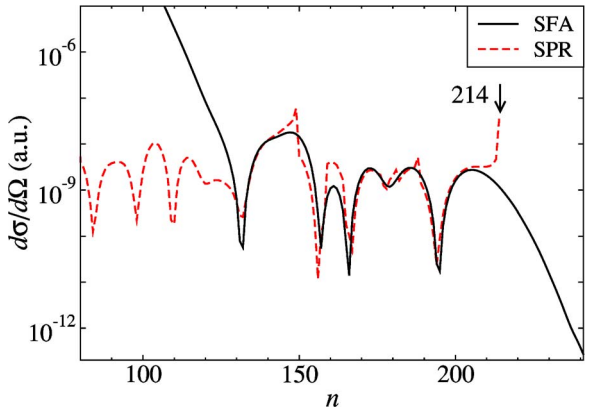

FIG. 5. (Color online) The rescattering part of the differential cross section as a function of the number of photons n exchanged with the laser field for the same laser, atomic, and the incident electron parameters as in Fig. 1. A comparison of the strong-field approximation (SFA—solid line) and the stationary phase approximation (SPR—dashed line).

$\tau > T/2$ are taken into account. The spikes on the dashed SPR curve are the consequence of the fact that the stationary phase method fails near the cutoff $n=n_{\mathrm{R}}^p$ of the respective pair of the stationary solution (see Fig. 4). Beyond the maximal of these cutoffs $n=n_{\mathrm{R}}=214$ there are no more real solutions.

For n close to n_{R}^p the stationary phase method fails and the uniform approximation for the rescattering T-matrix element has to be used [20]. The result is

$$T_{fi}^{\mathrm{R}}(n) \approx \sum_p [c_{n+}^p \mathrm{Ai}(\xi_n^p) + i c_{n-}^p \mathrm{Ai}'(\xi_n^p)] \times 2\pi^{3/2} \exp\{i\bar{S}_n^p + i\,\mathrm{sgn}[S_n^{tt}(t_s^p, \tau_s^p)]\pi/4\}, \quad (22)$$

where

$$\bar{S}_n^p = [S_n^{\mathrm{R}}(t_1^p, \tau_1^p) + S_n^{\mathrm{R}}(t_2^p, \tau_2^p)]/2,$$

$$\xi_n^p = -\{3[S_n^{\mathrm{R}}(t_1^p, \tau_1^p) - S_n^{\mathrm{R}}(t_2^p, \tau_2^p)]/4\}^{2/3}, \quad (23)$$

$$c_{n\pm}^p = \xi^{\pm 1/4}[f_n(t_1^p, \tau_1^p) \pm f_n(t_2^p, \tau_2^p)], \quad (24)$$

$$f_n(t,\tau) = \frac{2}{T}\left(\frac{\pi}{\tau}\right)^{3/2} \frac{(i-1)V_{\mathbf{k}_s-\mathbf{k}_f} V_{\mathbf{k}_i-\mathbf{k}_s}}{|\det[C_n(t,\tau)]|^{1/2}}. \quad (25)$$

For $n > n_{\mathrm{R}}^p$ there are no more real solutions of the saddle-point equations. However, the complex solutions exist and the $n > n_{\mathrm{R}}^p$ case can be treated similarly, as we have done for direct scattering. The complex rescattering saddle-point solutions and the uniform approximation were analyzed in Ref. [23] for high-order above-threshold ionization and in [24] for high-order harmonic generation. Here we use only the real rescattering solutions but, following the exponentially decreasing tendency of each particular contribution, we extrapolate each partial contribution beyond its cutoff at $n=n_{\mathrm{R}}^p$ and sum all them in Eq. (22). The results obtained using such modification of the uniform approximation with real solutions are compared with the SFA results in Fig. 1. The agreement is excellent.

The rescattering electron trajectory consists of three parts. The first two parts are the same as for the single scattering: for $t_i < t < t_s$ the trajectory is given by Eq. (13), while for $t_s < t < t_r$, with $t_r = t_s + \tau$, it is given by Eq. (14). The electron velocity at the moment of rescattering ($t=t_r$) is $\mathbf{v}(t_r) = \mathbf{A}(t_r) + \mathbf{A}(t_i) - 2\mathbf{A}(t_s) - \mathbf{k}_i$, so that the third part of the trajectory for $t > t_r$ is given by

$$\mathbf{r}(t) = \int_{t_r}^{t} dt' \mathbf{A}(t') + [\mathbf{k}_i + 2\mathbf{A}(t_s) - \mathbf{A}(t_i) - 2\mathbf{A}(t_r)](t - t_r) + \mathbf{r}(t_r), \quad (26)$$

where $\mathbf{r}(t_r) = \mathbf{0}$, and we have changed the sign of the electron velocity after the rescattering. In Fig. 3, besides the direct trajectories, the rescattering trajectories for $n=200$ (dotted and dot-dashed line) are shown. These trajectories correspond to the rescattering solutions having the highest maximum on Fig. 4, denoted by $p=1$. Since $n=200$ photons are absorbed from the laser field the final electron energy is much higher than in the case of the direct scattering. Similarly as for the direct scattering, the interferences appear since there are the two rescattering times t_{r1} and t_{r2} that contribute to the same final electron energy $E_{\mathbf{k}_f}$.

V. CONCLUSIONS AND COMMENTS

The laser-atom physics in the high-intensity and low-frequency regime combines quantum mechanics and classical physics in a unique fashion. This is the most visible in terms of Feynman's path integral: only few quantum orbits are enough to describe such processes satisfactorily. Quantum mechanics emerges through the tunneling and the interference of matter, while the classical mechanics is visible through the particle propagation and their trajectories. In the quantum-orbit formalism, both the time and the particle trajectories are complex. This is usually related to the tunneling nature of the ionization process in the strong field. Mathematically, this is expressed through the energy-conserving condition: the negative binding electron energy can be equal to the positive outgoing electron kinetic energy only if the time is complex.

In the present paper, we have shown that it is not always necessary to treat the times and orbits as complex. The saddle-point equations are usually connected with the energy-conserving conditions for each particular step of the laser-field-induced multistep process. There are many cases for which the real solutions of the saddle-point equations exist. In these cases the phases of the transition matrix elements, which correspond to these solutions, are also real. The coherent sum of all these matrix elements reproduces the quantum result obtained using the S-matrix formalism and the strong-field approximation. We have illustrated this using the example of the laser-assisted electron-atom scattering process. In this case, the initial electron energy is positive so that the real solutions are possible. The interference of these real solutions and the corresponding real electron trajectories is an example of how the quantum interference effects emerge from purely real trajectories that are the solutions of the Newton's equation of motion of the electron in the laser field. It is also shown that the real solutions can be used for the intermediate step of the process when one usually expects that only the complex solutions are applicable.

We consider the electrons having the same energy and the direction after leaving the region of the interaction with the laser field. There are two or more real electron trajectories with different emission (rescattering) times that correspond to these electrons. Their interference is visible in the electron spectrum. This can be related with the recent attosecond double-slit experiment in time [21].

ACKNOWLEDGMENTS

This work was supported in part by the Ministry of Education and Science, Canton Sarajevo, by the Federal Ministry of Education and Science, Bosnia and Herzegovina, by the VolkswagenStiftung, and by the NSERC Special Research Opportunity Program, Canada.

[1] W. Becker, F. Grasbon, R. Kopold, D. B. Milošević, G. G. Paulus, and H. Walther, Adv. At., Mol., Opt. Phys. **48**, 35 (2002).
[2] D. B. Milošević and F. Ehlotzky, Adv. At., Mol., Opt. Phys. **49**, 373 (2003).
[3] A. Becker and F. H. M. Faisal, J. Phys. B **38**, R1 (2005).
[4] L. V. Keldysh, Zh. Eksp. Teor. Fiz. **47**, 1945 (1964) [Sov. Phys. JETP **20**, 1307 (1965)].
[5] For the pioneering work about the so-called three-step model see, for example, P. B. Corkum, Phys. Rev. Lett. **71**, 1994 (1993), for high-order harmonic generation; and G. G. Paulus, W. Becker, W. Nicklich, and H. Walther, J. Phys. B **27**, L703 (1994), for high-order above-threshold ionization.
[6] P. Salières, B. Carré, L. Le Déroff, F. Grasbon, G. G. Paulus, H. Walther, R. Kopold, W. Becker, D. B. Milošević, A. Sanpera, and M. Lewenstein, Science **292**, 902 (2001).
[7] D. B. Milošević, D. Bauer, and W. Becker, J. Mod. Opt. **53**, 125 (2006).
[8] F. Ehlotzky, A. Jaroń, and J. Z. Kamińsky, Phys. Rep. **297**, 63 (1998).
[9] G. G. Paulus, F. Lindner, H. Walther, A. Baltuška, E. Goulielmakis, M. Lezius, and F. Krausz, Phys. Rev. Lett. **91**, 253004 (2003).
[10] D. B. Milošević, G. G. Paulus, and W. Becker, Opt. Express **11**, 1418 (2003); Laser Phys. Lett. **1**, 93 (2004).
[11] D. B. Milošević, G. G. Paulus, and W. Becker, Phys. Rev. A **71**, 061404(R) (2005).
[12] M. Busuladžić, A. Gazibegović-Busuladžić, and D. B. Milošević, Laser Phys. **16**, 289 (2006).
[13] D. B. Milošević, G. G. Paulus, D. Bauer, and W. Becker, "Above-threshold ionization by few-cycle pulses," J. Phys. B (topical review in preparation).
[14] A. Čerkić and D. B. Milošević, Phys. Rev. A **70**, 053402 (2004); Laser Phys. **15**, 268 (2005). See also N. L. Manakov, A. F. Starace, A. V. Flegel, and M. V. Frolov, Pis'ma Zh. Eksp. Teor. Fiz. **76**, 316 (2002) [JETP Lett. **76**, 258 (2002)]; A. V. Flegel, M. V. Frolov, N. L. Manakov, and A. F. Starace, Phys. Lett. A **334**, 197 (2005)
[15] There are various generalizations of the first Born approximation that include the higher-order terms of the Born expansion in the scattering potential $V(\mathbf{r})$. For example, this is the well-known low-frequency approximation: N. M. Kroll and K. M. Watson, Phys. Rev. A **8**, 804 (1973). For its generalization and explicit calculations see: D. B. Milošević, J. Phys. B **28**, 1869 (1995); **30**, 5251 (1997). However, such Born expansions in $V(\mathbf{r})$ are different from our SFA theory. In particular, they do not lead to the rescattering plateau observed in [14].
[16] M. V. Frolov, N. L. Manakov, E. A. Pronin, and A. F. Starace, Phys. Rev. Lett. **91**, 053003 (2003); D. Bauer, D. B. Milošević, and W. Becker, Phys. Rev. A **72**, 023415 (2005); B. Bergues, Y. Ni, H. Helm, and I. Yu. Kiyan, Phys. Rev. Lett. **95**, 263002 (2005).
[17] M. Abramowitz and I. A. Stegun, *Handbook of Mathematical Functions* (Dover, New York, 1964).
[18] F. V. Bunkin and M. V. Fedorov, Zh. Eksp. Teor. Fiz. **49**, 1215 (1965) [Sov. Phys. JETP **22**, 844 (1965)].
[19] N. Bleistein and R. A. Handelsman, *Asymptotic Expansions of Integrals* (Dover, New York, 1986).
[20] V. A. Borovikov, *Uniform Stationary Phase Method* (The Institution of Electrical Engineers, London, 1994).
[21] F. Lindner, M. G. Schätzel, H. Walther, A. Baltuška, E. Goulielmakis, F. Krausz, D. B. Milošević, D. Bauer, W. Becker, and G. G. Paulus, Phys. Rev. Lett. **95**, 040401 (2005).
[22] It is difficult to calculate the partial contributions of these solutions since both the stationary phase and the uniform approximation for the case of two coalescing points fail. In the case of three close stationary points the results can be expressed in terms of the Piercey integral [20].
[23] C. Figueira de Morisson Faria, H. Schomerus, and W. Becker, Phys. Rev. A **66**, 043413 (2002).
[24] D. B. Milošević and W. Becker, Phys. Rev. A **66**, 063417 (2002); S. Odžak and D. B. Milošević, *ibid.* **72**, 033407 (2005).